

Using Computational Fluid Dynamics in the Determination of Solar Collector Orientation and Stack Height of a Solar Induced Ventilation Prototype

Yusoff, W. F. M.^{1*}, Sopian, A. R.², Salleh, E.³, Adam, N. M.⁴, Hamzah, Z.¹ and Mamat, M. H. H.⁵

¹Department of Architecture, Faculty of Engineering and Built Environment, Universiti Kebangsaan Malaysia, 43600 Bangi, Selangor, Malaysia

²Department of Architecture, Kulliyah of Architecture and Environmental Design, International Islamic University Malaysia, P.O. Box 10, 50728 Kuala Lumpur, Malaysia

³Solar Energy Research Institute, Level 3, Perpustakaan Tun Sri Lanang, Universiti Kebangsaan Malaysia, 43600 Bangi, Selangor, Malaysia

⁴Department of Mechanical and Manufacturing Engineering, Faculty of Engineering, Universiti Putra Malaysia, 43400 Serdang, Selangor, Malaysia

⁵Department of Operations and Manufacturing, TPM Engineering Sdn. Bhd, Technology Park Malaysia, Lebuhraya Puchong-Sg Besi, Bukit Jalil, 57000 Kuala Lumpur, Malaysia

ABSTRACT

Stack ventilation in the hot and humid climate is inherently inefficient due to minimal air temperature differences between indoor and outdoor environment of a naturally ventilated building. Solar induced ventilation is a viable alternative in enhancing this stack ventilation. This paper aims to demonstrate investigations on the effective solar collector orientation and stack height for a solar induced ventilation prototype that utilizes roof solar collector and vertical stack. The orientation of the solar collector is significant as it determines the amount of solar radiation absorbed by the solar collector. Meanwhile, the height of the vertical stack influences the creation of the stack pressure in inducing air movement. Investigations were executed using a simulation modelling software called FloVENT. The validation of the simulation modelling against physical experiment indicated a good agreement between these two results. Analyses were executed on the air temperature increments inside the solar collector. A

high increment of the air temperature resulted in the effective orientation. Meanwhile, the air temperature and mass flow rate of the various heights of the vertical stack were also analyzed. The findings concluded that the recommended orientation for the prototype's solar collector is the west-facing orientation. It was also found that the higher the vertical stack, the lower the air temperature inside the stack would be, but with greater induced mass flow rate.

Article history:

Received: 18 May 2011

Accepted: 18 June 2012

E-mail addresses:

wardahyusoff@gmail.com (Yusoff, W. F. M.),

arazaks@iium.edu.my (Sopian, A. R.),

elsall06@gmail.com (Salleh, E.),

mariah@upm.edu.my (Adam, N. M.),

zh.akitek@gmail.com (Hamzah, Z.),

intelligentmove@gmail.com (Mamat, M. H. H.)

*Corresponding Author

Keywords: Height, hot and humid climate, orientation, roof solar collector, solar induced ventilation, vertical stack

INTRODUCTION

Solar induced ventilation studies have been gaining interest due to the strategy's potential in enhancing stack ventilation. The configuration normally consists of a glass cover, an air cavity and an absorber plate or wall. Solar radiation is used to heat up the absorber plate or wall. The heat from the absorber plate or wall, as well as the glass cover, is transferred to the air inside the cavity through convective heat transfer. Consequently, high air temperature differences between the air inside the cavity and the ambient air develops. The solar induced ventilation strategies that have been widely investigated are Trombe wall, solar chimney and roof solar collector (Awbi, 2003). Although they have similar operating concept, their configurations are somehow different. While the Trombe wall and solar chimney have vertical air cavity, the roof solar collector's air cavity is inclined and normally follows the roof slope.

Many studies have been carried out on the configurations of solar induced ventilation (see Bouchair, 1994; Chen *et al.*, 2003; Ding *et al.*, 2005; Gan, 2006; Hamdy & Fikry, 1998; Li *et al.*, 2004; Mathur *et al.*, 2006; Miyazaki *et al.*, 2006; Susanti *et al.*, 2008). The configuration parameters investigated were height, length, cavity width, tilt angle and opening sizes. The purpose of the studies was to enhance the performance of the solar induced ventilation. The investigations on the correlations between the cavity width and the inlet size showed that friction loss dominated in a small cavity width, whilst the pressure loss dominated in a small inlet size (Miyazaki *et al.*, 2006). Despite this, a simultaneous increase in both the cavity width and the inlet size resulted in no optimum cavity width, as there was no air flow rate reduction (Chen *et al.*, 2003; Gan, 2006).

The correlation between the cavity width and the stack height resulted in the effective ratio of 1:10 (Bouchair, 1994; Gan 2006; Li *et al.*, 2004). However, this correlation was investigated for solar induced ventilations with a vertical stack, namely, Trombe wall and solar chimney. Meanwhile, the height study that excluded this correlation indicated that the higher the stack, the greater the induced air flow rate (Ding *et al.*, 2005). The performance of solar induced ventilation is also affected by tilt angle and opening sizes. The effective tilt angle was found to be various, depending on the location's latitude. This is due to the different solar altitude with different latitudes. The optimum tilt angle for Jaipur, India, (27°N latitude) during the summer months was 45° (Mathur *et al.*, 2006). Meanwhile, for 32°N latitude, the optimum tilt angle was 60° (Hamdy & Fikry, 1998). For the opening sizes, the ratio of 1 (ratio of inlet area to outlet area) was recommended in inducing high air flow rate (Susanti *et al.*, 2008).

The configuration studies mentioned above were executed for Trombe wall, solar chimney and roof solar collector. In this research, the configuration of the proposed solar induced ventilation is slightly different from those strategies. The solar induced ventilation proposed consists of two parts, which are the roof solar collector and the vertical stack. Roof solar collector has the advantage of collecting more solar radiation when the sun altitude is high, as compared to Trombe wall and solar chimney (Awbi, 2003; Mathur *et al.*, 2006). However,

its drawback is the height restriction of the stack, which is caused by the roof slope (Awbi, 2003; Harris & Helwig, 2007). Hence, the purpose of utilizing vertical stack is to increase the stack height, and consequently enhance the stack pressure. The proposed strategy has shown the potential in enhancing the stack ventilation in the hot and humid climate. For instance, the highest air temperature differences between the stack air and the ambient air attained by the proposed strategy was 9.9°C for 877 W/m² solar radiation incidents (Yusoff *et al.*, 2010).

Due to its potential, this study was carried out with the aim to enhance the performance of the proposed strategy by investigating the orientation of the solar collector and the height of the vertical stack. These two parameters are significant as they affect the induced ventilation of the strategy. The solar collector orientation influences the catchment of solar radiation, whereas the vertical stack height affects the development of the stack pressure. Although there are studies on the effective solar collector orientation for the northern hemisphere countries, they are only conducted for inclined solar collector (Bari, 2001; Gunerhan & Hepbasli, 2007; Shariah *et al.*, 2002) and vertical solar chimney (Nugroho, 2007). The investigation of an effective solar collector orientation for the proposed strategy in the northern hemisphere countries, particularly Malaysia, is yet to be conducted. Meanwhile, the vertical stack of the proposed strategy is not used for collecting solar radiation. Hence, it is assumed that there is convective heat loss from the induced air to the stack walls. For this reason, the investigations were executed to determine whether height affects air temperature and mass flow rate inside the vertical stack.

This paper is divided into five sections. The first section reviews on the previous studies of solar induced ventilation configuration and briefly describes the present research. The second section describes the solar induced ventilation prototype investigated in this paper. The third section presents the methodology employed, which is, simulation modelling. This section also elaborates on the prototype model, simulation set-up and procedures, simulation conditions, and simulation validation. Section four discusses the results of the investigations. This section is divided into two sub-sections, which are, the results of the solar collector orientation and the vertical stack height studies. Finally, the overall findings of the research are concluded in section five.

THE SOLAR INDUCED VENTILATION PROTOTYPE

The solar induced ventilation prototype investigated in this paper utilized a roof solar collector and a vertical stack (see Fig.1). The roof solar collector functioned as the solar radiation absorber and heater of the air inside the solar collector's cavity. The vertical stack functioned as a conventional chimney, without solar radiation collection. It provided a significant height in developing a sufficient stack pressure. The walls of the vertical stack were insulated all around in minimizing the heat gains and losses. This created air temperature differences and hence, pressure differences between the air inside the solar collector's cavity and the stack air. Consequently, the heated air inside the roof solar collector rose and flowed into the vertical stack. The inlet was located at the bottom of the roof solar collector, whilst the outlets were situated at the top of the vertical stack (Fig.1). There were obstructions placed at a distance of 0.15 m from the vertical stack outlets. These obstructions functioned as windbreakers that reduced the wind effects at the outlets. Without these obstructions, the induced air at the vertical stack outlets would be greatly affected by wind (Yusoff *et al.*, 2010).

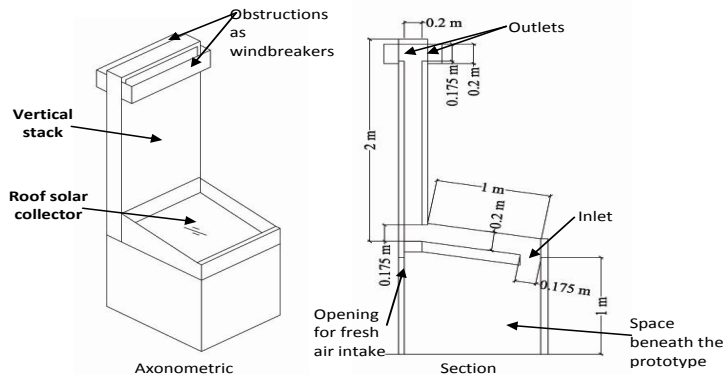


Fig.1: The prototype developed for the simulations

METHODOLOGY

The methodology employed in this study was simulation modelling using Computational Fluid Dynamic (CFD) software FloVENT version 9.1. The feasibility of FloVENT for natural convection studies had been proven by previous research (see Manz, 2003; Nugroho, 2007). In this study, the parameters considered were the prototype model, the simulation set-up and procedures, the simulation conditions and the validation of simulation modelling.

Prototype Model

The proposed prototype utilized a roof solar collector (RSC) and a vertical stack, as shown in Fig.1. The roof solar collector comprised of a glass cover, an air cavity and an absorber, while the vertical stack consisted of an air cavity and surrounded by insulated walls. The dimensions of the roof solar collector were 1 m x 1 m x 0.2 m (length x width x cavity width), whilst for the vertical stack the dimensions were 1 m x 2 m x 0.2 m (width x height x cavity width). There were obstructions made of plywood (1 m length x 0.2 m high), which were placed at a distance of 0.15 m from the vertical stack outlets.

The materials assigned to the prototype were a piece of black painted aluminium for the absorber, a clear glass for the top cover, and a plywood wall with insulations in the inner lining of the walls (Fig.2). The insulations were then covered with aluminium foil in reducing the radiative heat transfer between the walls' internal surfaces. The walls' external surfaces were also finished with aluminium foil to reduce the solar radiation absorption. The space beneath the prototype was fully covered to reduce the wind effects. However, openings were provided at one of the walls in allowing airflow into the space (Fig.1).

The orientation study utilized the prototype that had 2 meter high vertical stack. Meanwhile, for the height investigations, prototypes with three different vertical stack heights (2 m, 3 m and 4 m) were developed (Fig.3). The maximum height was 4 m, as the prototype was developed for application in a single storey industrial building; hence, it was deemed to be proportionate to the building typology applied. Other configurations which were the length and the tilt angle of the roof solar collector's channel, the cavity width and the opening areas (inlet and outlet)

were not investigated as they were derived from the literature review. In the literature, the recommended roof solar collector's channel length was 1 m, as no significant increment in the air temperature was obtained for the length greater than 1 m (Khedari *et al.*, 1997; Zhai *et al.*, 2005), and the suggested tilt angle for solar collector in Selangor, Malaysia was 10°. The cavity width of 0.2 m was utilized as the smaller the size (such as 0.1 m) would only increase the friction loss inside it (Bouchair, 1994; Miyazaki *et al.*, 2006), whereas a larger size would reduce the exit air temperature (Yousef, 2007). The inlet and outlet opening areas of the roof solar collector and vertical stack were of equivalent size, which was 0.1575 m² (0.9 m x 0.175 m). The purpose was to achieve the suggested effective ratio of 1:1 (inlet area:outlet area) for the opening areas (Khedari *et al.*, 2000; Susanti *et al.*, 2008).

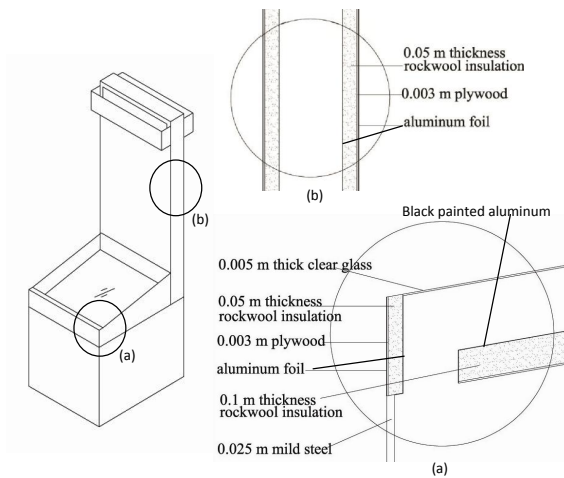


Fig.2: Materials of the prototype

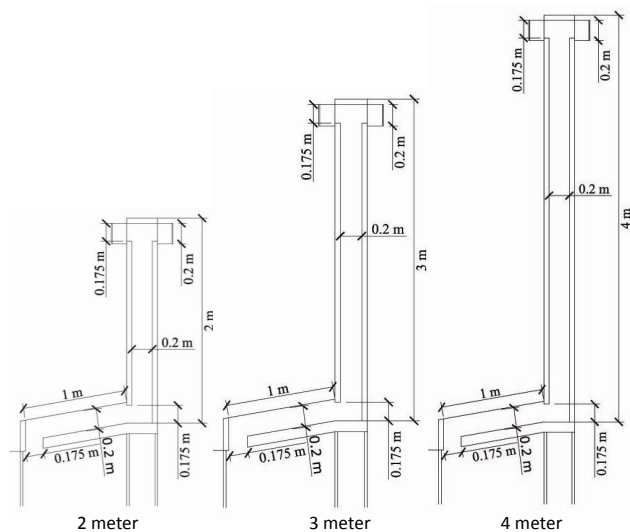


Fig.3: Prototypes with the different vertical stack heights

General Simulation Set-Up and Procedures

The prototype was placed in a solution domain which had a size of 7 m length x 7 m width x 6 m high. Its position was 3 m from x-plane, 3 m from z-plane and 0 m from y-plane (Fig.4). FloVENT version 9.1 provided three solution types, namely, the flow and heat transfer, the flow only and the conduction only. Since the investigations involved buoyancy induced ventilation, the solution type selected was the flow and heat transfer. Besides, the simulations also employed a steady state and three dimensional flow analyses. It also utilized Boussinesq approximation in solving the conservation equations. The flow regime was considered turbulence. There were three turbulence models available in FloVENT version 9.1, namely, the Capped LVEL, the LVEL Algebraic and the LVEL K-Epsilon. The simulations used the LVEL K-Epsilon turbulence model as it was the most appropriate for the built environment as compared to the others. This turbulence model utilized $k-\epsilon$ (the turbulent kinetic energy (k) and turbulent dissipation rate (ϵ)) approach in the calculation (Gan, 2006). The fluid applied in the simulations was air at 30°C, which had the following properties: conductivity was 0.02643 W/mK, viscosity was 1.872E-005 Ns/m², density was 1.149 kg/m³, and specific heat was 1007 J/kgK. The simulations used the Cartesian grid system. The outer iterations set for the simulations were 4000. Nevertheless, the simulation stopped automatically when it had attained convergence, even if the numbers set were not reached yet. Hence, the precise setting of outer iteration numbers was not critical (Mentor Graphics, 2010). The simulations also employed solar radiation calculation, in which the required input data were site latitude, simulation day, solar time and solar intensity. Meanwhile, the Atmospheric Boundary Layer (ABL) was applied in having the wind effects. The ABL was downloaded from the FloVENT website. It used Log Law model in generating the required wind profile. The north direction was set to be in the positive x direction.

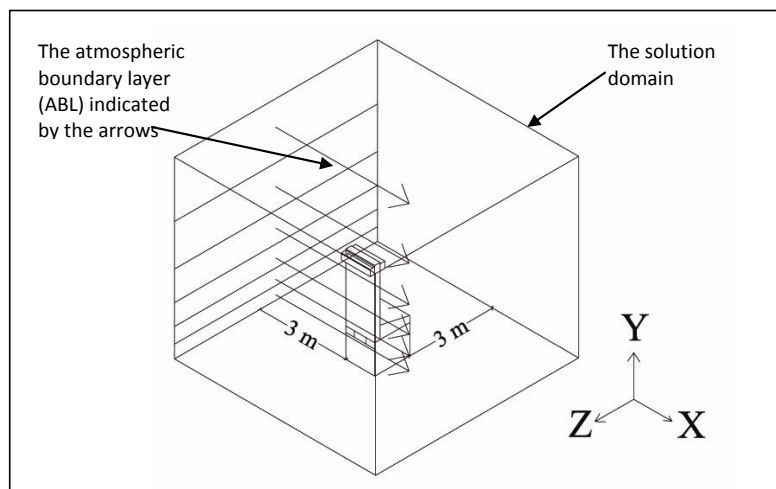


Fig.4: The position of prototype in the overall solution domain. Example is given for west orientation

Simulation Set-Up and Procedures for Orientation Study

The solar collector was oriented towards north, south, east and west. The effective orientation of solar collector was determined by the air temperature increment inside the RSC. This air temperature increment was calculated by the difference in the values between the monitor points at the RSC inlet and the vertical stack inlet. The locations of these monitor points are depicted in Fig.5.

Simulation Set-Up and Procedures for Height Study

In the investigations of vertical stack height, the prototype was oriented towards west, which was resulted from the orientation study. The variables investigated were air temperature and mass flow rate inside the vertical stack. Therefore, the monitor points were positioned at the inlet, middle and outlet of the vertical stack. The locations of monitor points are illustrated in Fig.5.

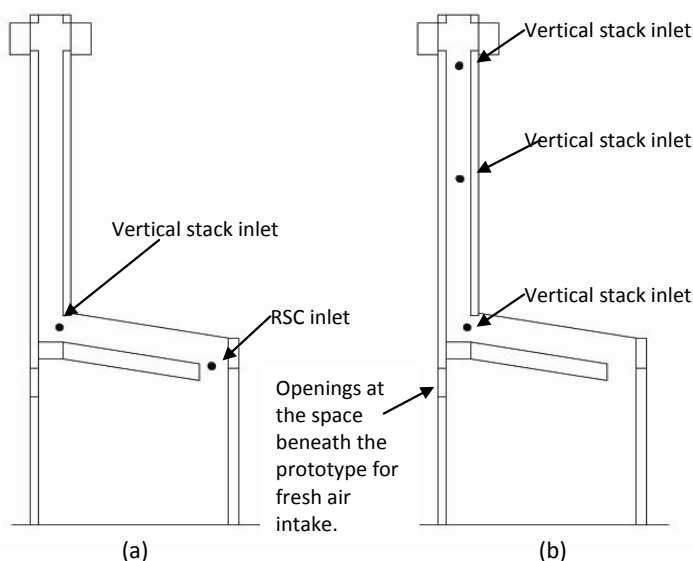


Fig.5: The location of monitor points at the prototype for solar collector orientation (a) and vertical stack height (b) studies

General Simulation Conditions

The initial boundary conditions employed the average of three years (2006-2008) environmental data from Subang weather station. The weather station is located at an airport formerly known as Sultan Abdul Aziz Shah (SAAS) airport, which is located in Selangor, Malaysia.

Simulation Conditions for Orientation Study

For the orientation study, the air temperature and solar radiation were the average data gathered on the 21 March, 22 June, 23 September and 21 December. These dates were selected as they represent the equinoxes and solstices. Meanwhile, the data utilized for wind speed and

wind direction were the annual average data. The purpose was to reduce the variability of the environmental parameters input data. The wind speed data of Subang weather station was corrected to a reference height of 1.6 m. The annual prevailing wind directions were north, northwest and south. However, the simulations utilized wind direction from south (180°) for ease of comparison. The selected times for solar collector orientation study were 10 a.m., 12 p.m. and 2 p.m. These times represented the morning, noon and evening hours.

Simulation Conditions for Height Study

The investigations of the vertical stack height employed the average data on the 21 March. March was selected as it was the month with the highest monthly mean solar radiation recorded for 20 years (1988-2008) by Subang weather station. Similar to orientation study, the wind speed data of Subang weather station was corrected to a reference height of 1.6 m. The prevailing wind direction in March was northwest. However, the simulations utilized annual prevailing wind direction which was south, as downward flow occurred inside the vertical stack for simulations using northwest wind direction. This downward flow hindered the investigations of height effects to the air temperature and mass flow rate inside the vertical stack. The selected times for the investigations were 12 p.m. and 2 p.m. only. No simulations were executed during morning hours because the west facing prototype had caused downward flow inside the vertical stack during this time.

Validation of Simulation Modelling

The simulation modelling was validated against physical experiment by Yusoff *et al.* (Mentor Graphics, 2010). Tables 1 and 2 depict the deviation percentage at each point's location from 9 a.m. to 4 p.m. The variables validated were air temperature and velocity. The air temperature was validated at six locations, namely, the RSC inlet, RSC 1, RSC 2, vertical stack inlet, vertical stack middle, and vertical stack outlet. Meanwhile, the air velocity was validated at three locations, which were the RSC inlet, vertical stack inlet and vertical stack outlet. The validation between the simulation modelling and physical experiment indicated a good agreement between the two results. The total average air temperature deviation for six

TABLE 1
The percentage of deviations for air temperature at six locations

Monitor points' Locations	Time (h)								Average deviation (%)
	9	10	11	12	1	2	3	4	
RSC inlet	0	2	1	4	2	1	4	5	2
RSC 1	12	15	11	7	12	11	9	6	10
RSC 2	13	17	12	7	14	12	10	10	12
V. stack inlet	11	13	11	0	8	10	10	8	9
V. stack middle	5	9	6	2	8	8	7	11	7
V. stack outlet	2	7	4	2	3	2	0	6	3

TABLE 2
The percentage of deviations for air velocity at three locations

Monitor points' Locations	Time (h)								Average deviation (%)
	9	10	11	12	1	2	3	4	
RSC inlet	28	12	10	18	18	15	4	13	15
V. stack inlet	21	7	1	2	17	14	15	5	10
V. stack outlet	10	5	16	17	18	17	20	11	14

locations was 7%, with maximum average deviation of 12% at RSC 2 (Table 1). Meanwhile, the total average deviation for air velocity at three locations was 13%, with the maximum average deviation of 15% at RSC inlet (Table 2).

RESULTS AND DISCUSSION

The results are presented and discussed in two sub-sections, which are the effective solar collector orientation and the effects of vertical stack height to the air temperature and mass flow rate.

Effective Orientation of the Prototype's Solar Collector

Fig.6 depicts the air temperature increments at three separate times, which were 10 a.m., 12 p.m. and 2 p.m., attained by the prototype for the particular orientations and on the particular dates. The results showed that the most effective solar collector orientation at 10 a.m. for all dates was east. At 2 p.m., the effective orientations on the 22 June and 21 December were west and south, respectively. Meanwhile, on the 21 March and 23 September, it could be either west or south. At 12 p.m., the effective solar collector orientations on the 22 June were east and west, whilst on the 21 December, it was south. However, the effective solar collector orientation at 12 pm on the 21 March and 23 September could be south, east or west.

Similarly, Fig.7 depicts the average air temperature increment at three separate times, namely, 10 a.m., 12 p.m. and 2 p.m. that was achieved by the prototype. The air temperature increments determined the orientation effectiveness, in which a high increment resulted in the effective orientation. The results indicated that the highest air temperature increment on the 22 June was attained by the west orientation. Meanwhile for the remaining three dates (namely, the 21 December, 21 March and 23 September), the highest air temperature increment was achieved by the south orientation. It is also apparent from Fig.7 that the most ineffective orientation for the prototype's solar collector was the north.

In summary, the suggested effective orientation for the prototype's solar collector throughout the year was west. However, it was emphasized that the west orientation might be effective for the proposed prototype only, as it had different configuration compared to the vertical solar chimney (Nugroho, 2007) and inclined solar collector (Bari, 2001; Gunerhan & Hepbasli, 2007; Shariah *et al.*, 2002), as described in the literature. The west orientation was recommended instead of the south because the air temperature increment in June for the south

orientation was very poor (Fig.7), especially at 12 p.m. (Fig.6). The sun path in June caused the vertical stack to shade the south facing solar collector, as shown in Fig.8. The prototype's solar collector was essential to attain a significant air temperature increment in June, as it was the hottest month compared to the others. The 20 years (1988-2008) monthly average weather data by Subang weather station indicated that the average ambient air temperature in June was 28°C. It was the highest compared to December (26.8°C), March (27.8°C) and September (27.4°C). Moreover, the monthly mean solar radiation received in June was also higher than in December.

Fig.7 also shows that the air temperature increments for the south orientation in December, March and September were in the average of 2°C higher than the west orientation. In June, however, the air temperature increment of the west orientation was 3.95°C higher than the south orientation. The results also indicated that the average air temperature increments at 12 p.m. and 2 p.m. of the south orientation was almost equal to the west orientation in March and September, 1°C higher in December, but 7°C lower in June (Fig.6). Meanwhile, the comparison between the east and west orientation showed that higher air temperature increment was attained by the west orientation in all months, except in September (Fig.7).

The drawback of orientating the prototype's solar collector to the west was the poor collection of solar radiation in the morning. This is due to the morning sun path which caused the vertical stack to shade the west facing solar collector, as shown in Fig.9. This phenomenon also resulted in no air temperature increment in the prototype's solar collector at 10 a.m. in March and September, as shown in Fig.6. Consequently, downward flow occurred inside the prototype.

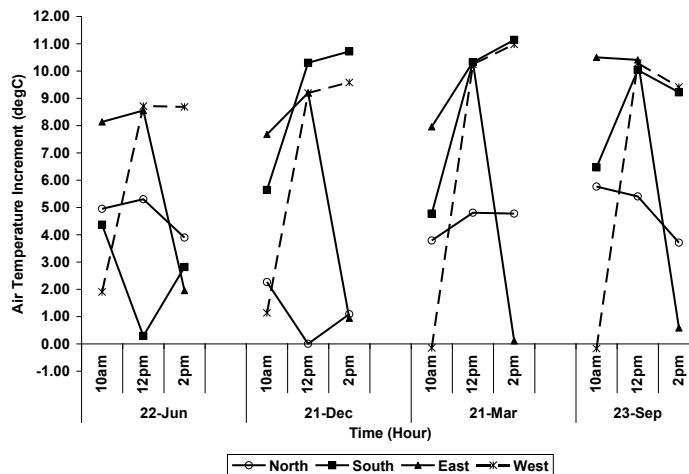


Fig.6: The air temperature increments at 10 a.m., 12 p.m. and 2 p.m. for the north, south, east and west orientations on the 22 June, 21 December, 21 March and 23 September

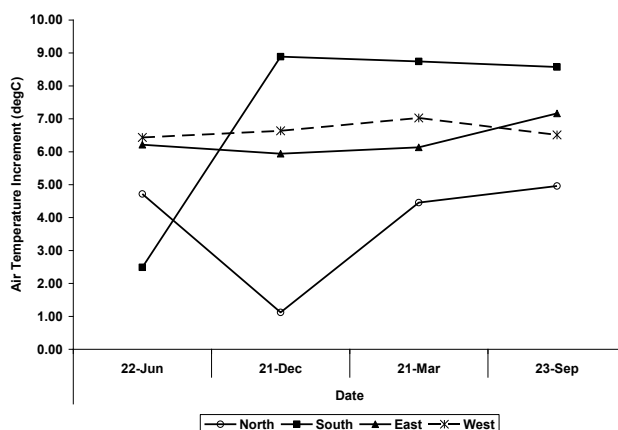


Fig.7: The average air temperature increments for the north, south, east and west orientations on the 22 June, 21 December, 21 March and 23 September

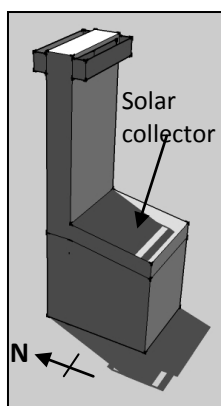


Fig.8: The south facing of the prototype’s solar collector as at 12 p.m. on the 22 June

Although the west orientation resulted in a poor collection of solar radiation in the morning (Fig.6), the need for the prototype to induce more ventilation rate at noon and evening hours was more critical compared to the morning hours due to the higher indoor air temperature. Investigations into Malaysian single storey terrace houses showed that from the morning to noon hours, the indoor air temperature was almost equal to the outdoor air temperature. However, in the evening (i.e., from 3 p.m. to 7 p.m.), the indoor air temperature was 2 to 3°C higher than the outdoor air temperature. Meanwhile, the PMV analysis of the master bedroom indicated that the PMV value was below +1.5 from 8 a.m. to 11 a.m., whereas from 1 p.m. to 3 p.m., the PMV value was +1.5 and above. The highest PMV value of +2 was achieved at 12 p.m. (Nugroho *et al.*, 2007).

In this research, comparisons of comfort condition between 10 a.m. and 2 p.m. were executed using the indoor predicted comfort temperature equations by Nicol and Humphreys (2010), as follows:

$$T_c = 13.5 + 0.54T_o \quad [1]$$

Where T_c was the indoor predicted comfort temperature and T_o was the monthly mean outdoor air temperature. The comparisons showed that the indoor predicted comfort temperature (T_c) was relatively closer to the monthly mean outdoor air temperature (T_o) at 10 a.m. compared to 2 p.m., except in September where the values were equal (Fig.10). In March, the monthly mean outdoor air temperature (T_o) was 0.6°C lower than the indoor predicted comfort temperature (T_c) at 10 a.m. At 2 p.m., the monthly mean outdoor air temperature (T_o) was 1.2°C higher than the indoor predicted comfort temperature (T_c). In June, the monthly mean outdoor air temperature (T_o) was higher than the indoor predicted comfort temperature (T_c) at both 10 a.m. (0.2°C) and 12 p.m. (1°C). Meanwhile in December, the comparisons showed that the monthly mean outdoor air temperature (T_o) was 0.3°C lower at 10 a.m. and 0.9°C higher at 2 p.m. than the indoor predicted comfort temperature (T_c).

Height of the Vertical Stack

It is apparent from the results obtained in Fig.11 that the higher the vertical stack was, the lower the air temperature inside the stack. The 2 m high vertical stack had the highest air temperature at all the monitor points. Meanwhile, the air temperature profiles were similar for all heights, in which the highest air temperature was attained at the vertical stack inlet. The air temperature decreased at the middle of the vertical stack and increased again when approaching the vertical stack outlet. The possible explanation to this phenomenon was due to the convective heat gain and loss of the air inside the prototype. The air at the vertical stack inlet had the highest temperature as it was heated inside the RSC. As the heated air rose and flowed upward inside the vertical stack, it experienced convective heat loss to the stack walls, which caused lower air temperature at the middle of the stack. However, at certain a height inside the vertical stack, the air temperature might be lower than the stack wall's temperature. Hence, the air experienced convective heat gain from the stack walls. This might explain the increase of air temperature from the middle to the outlet of the stack.

Fig.12 shows the mass flow rate at the inlet, middle and outlet of the 2 m, 3 m and 4 m high vertical stack. The mass flow rate results were in reverse to the air temperature results, in which the higher the vertical stack was, the greater the mass flow rate. However, there was no significant difference of the induced mass flow rate at the vertical stack inlet of all the heights compared to the middle and outlet of the stack. This finding showed that the stack pressure developed with the stack height. Another important finding was that the increase of mass flow rate from the inlet to the middle of the stack was higher than from the middle to the outlet. Moreover, at 12 p.m., there was a decrease in the mass flow rate from the middle to the outlet for the 2 m high vertical stack. This might be related to the air temperature inside the vertical stack. Besides the height, the stack pressure was also influenced by the air temperature. The higher the air temperature inside the stack a greater stack pressure is implied (2002). The air

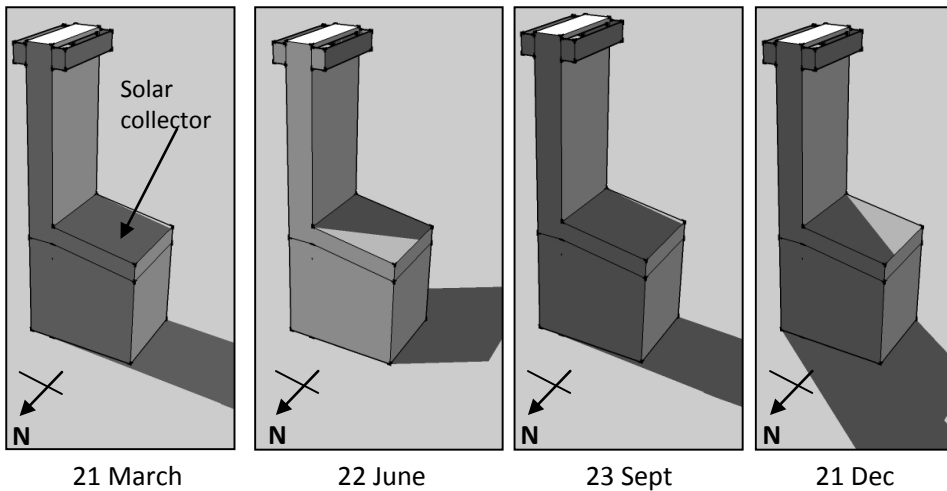


Fig.9: The west facing of the prototype’s solar collector as at 10 a.m. on the 21 March, 22 June, 23 September and 21 December

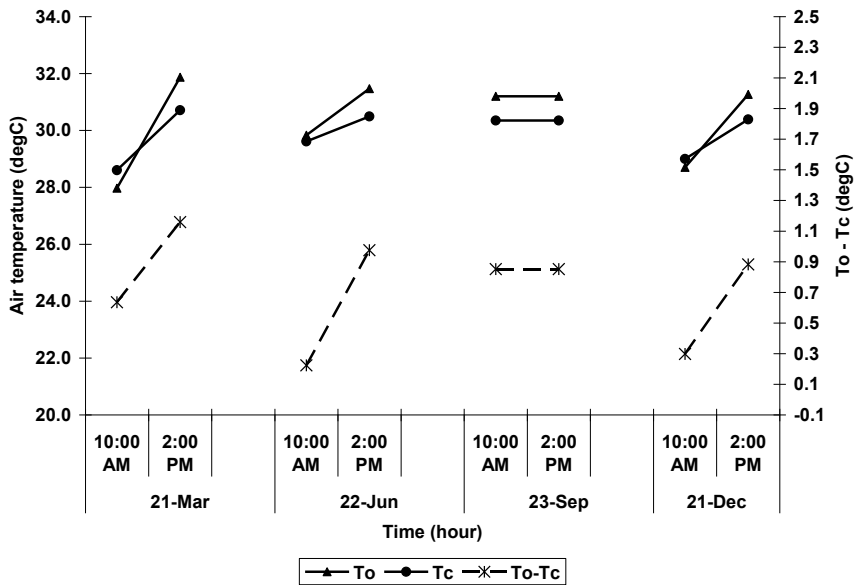


Fig.10: The comparison of comfort conditions between 10 a.m. and 2 p.m.

temperature at the inlet was the highest compared to the other part inside the vertical stack as it had just been heated inside the roof solar collector. As it flowed upwards, it experienced the heat gain and loss inside the stack. The reduction in the air temperature caused the lower increment of mass flow rate from the middle to the outlet compared from the inlet to the middle of the stack.

In summary, the higher the stack was, the lower the air temperature, but with a greater induced mass flow rate. Although the air temperature experienced more heat loss with the increase of stack height, the increase in stack pressure enabled the prototype to induce a higher mass flow rate.

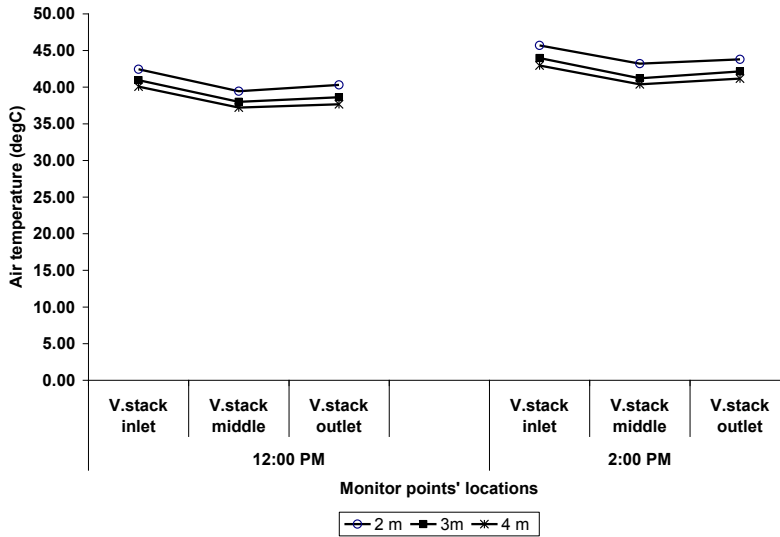


Fig.11: The air temperature inside the 2 m, 3 m and 4 m high vertical stack at 12 p.m. and 2 p.m.

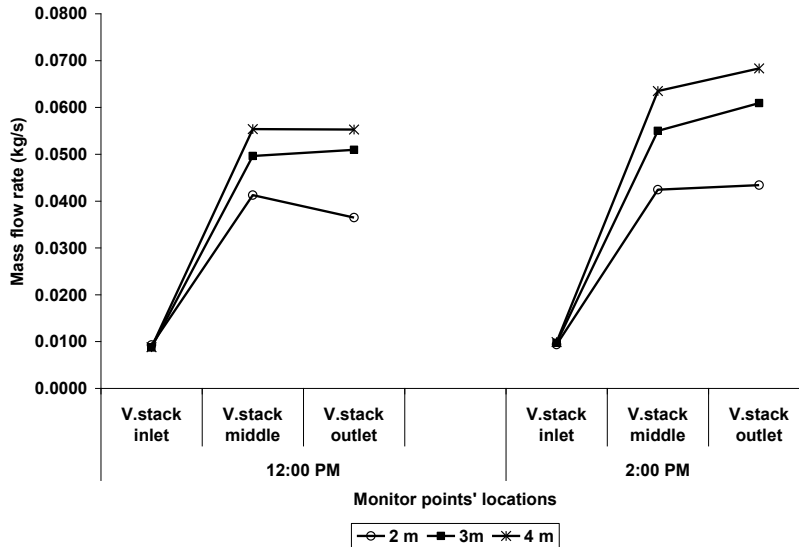


Fig.12: The mass flow rate inside the 2 m, 3 m and 4 m high vertical stack at 12 p.m. and 2 p.m.

CONCLUSION

This study investigated the solar collector orientation and vertical stack height for solar induced ventilation that utilized roof solar collector and vertical stack using simulation modelling. The validation of simulation modelling against physical experiment had shown a positive agreement between the two results. The study concluded that the effective solar collector orientation throughout the year for the prototype in the northern hemisphere countries, particularly in Malaysia, is the west. Hence, the suggested orientation is not in conformity with the findings from the literatures, which recommended south as the effective solar collector orientation throughout the year for the northern hemisphere countries (Bari, 2001; Gunerhan & Hepbasli, 2007; Nugroho, 2007; Shariah *et al.*, 2002). The different finding is due to the different configurations of the prototype, in which the vertical stack has caused shading to the south facing solar collector in June. The study also concluded that the higher the vertical stack is, the lower the air temperature, but the greater the induced mass flow rate. In summary, the investigations confirmed the potential of the proposed solar induced ventilation for the application in the hot and humid climate. Therefore, it would be interesting to examine the effects of the proposed solar induced ventilation to the indoor air temperature and ventilation rates for buildings in future research undertakings.

ACKNOWLEDGEMENTS

The authors would like to thank the International Islamic University Malaysia for the endowment of research grant (EDW B 1001-345) that enabled the purchasing of the CFD software.

REFERENCES

- Awbi, H. B. (2003). *Ventilation of Buildings* (2nd Edition). London: Spon Press.
- Bari, S. (2001). Optimum orientation of domestic solar water heaters for the low latitude countries. *Energy Conversion and Management*, 42(10), 1205-1214.
- Bouchair, A. (1994). Solar chimney for promoting cooling ventilation in Southern Algeria. *Building Services Engineering Research and Technology*, 15(2), 81-93.
- Chen, Z. D., Bandopadhyay, P., Halldorsson, J., Byrjalsen, C., Heiselberg, P., & Li, Y. (2003). An experimental investigation of a solar chimney model with uniform wall heat flux. *Building and Environment*, 38(7), 893-906.
- Ding, W., Hasemi, Y., & Yamada, T. (2005). Natural ventilation performance of a double-skin façade with a solar chimney. *Energy and Buildings*, 37(4), 411-418.
- Gan, G. (2006). Simulation of buoyancy-induced flow in open cavities for natural ventilation. *Energy and Buildings*, 38(5), 410-420.
- Gunerhan, H., & Hepbasli, A. (2007). Determination of the optimum tilt angle of solar collectors for building applications. *Building and Environment*, 42(2), 779-783.
- Hamdy, I. F., & Fikry, M. A. (1998). Passive solar ventilation. *Renewable Energy*, 14(1-4), 381-386.

- Harris, D. J., & Helwig, N. (2007). Solar chimney and building ventilation. *Applied Energy*, 84(2), 135-146.
- Khedari, J., Hirunlabh, J., & Bunnag, T. (1997). Experimental study of a roof solar collector towards the natural ventilation of new houses. *Energy and Buildings*, 26(2), 159-164.
- Khedari, J., Mansirisub, W., Chaima, S., Pratinthong, N., & Hirunlabh, J. (2000). Field measurements of performance of roof solar collector. *Energy and Buildings*, 31(3), 171-178.
- Li, A., Jones, P., Zhao, P., & Wang, L. (2004). Heat transfer and natural ventilation airflow rates from single-sided heated solar chimney for buildings. *Asian Architecture and Building Engineering*, 3(2), 233-238.
- Manz, H. (2003). Numerical simulation of heat transfer by natural convection in cavities of facade elements. *Energy and Buildings*, 35(3), 305-311.
- Mathur, J., Mathur, S., & Anupma (2006). Summer-performance of inclined roof solar chimney for natural ventilation. *Energy and Buildings*, 38(10), 1156-1163.
- Mentor Graphics (2010). *FloVENT® User Guide-Software Version 9.1*.
- Miyazaki, T., Akisawa, A., & Kashiwagi, T. (2006). The effects of solar chimneys on thermal load mitigation of office buildings under the Japanese climate. *Renewable Energy*, 31(7), 987-1010.
- Nicol, J. F., & Humphreys, M. A. (2002). Adaptive thermal comfort and sustainable thermal standards for buildings. *Energy and Buildings*, 34(6), 563-572.
- Nugroho, A. M. (2007). *Solar Chimney Geometry for Stack Ventilation in Malaysia Terrace House*. (Doctoral dissertation). Universiti Teknologi Malaysia, Johor.
- Nugroho, A. M., Hamdan, M., & Ossen, D. R. (2007). A preliminary study of thermal comfort in Malaysia's single storey terraced houses. *Asian Architecture and Building Engineering*, 182, 289-296.
- Shariah, A., Al-Akhras, M. A., & Al-Omari, I. A. (2002). Optimizing the tilt angle of solar collectors. *Renewable Energy*, 26(4), 587-598.
- Susanti, L., Homma, H., Matsumoto, H., Suzuki, Y., & Shimizu, M. (2008). A laboratory experiment on natural ventilation through a roof cavity for reduction of solar heat gain. *Energy and Buildings*, 40(12), 2196-2206.
- Yousef, B. A.-R. A. A. A. (2007). *Development of a Mathematical Model to Predict Thermal Performance and Cost Effectiveness of Solar Air Heaters*. Doctoral dissertation, Universiti Putra Malaysia, Selangor.
- Yusoff, W. F. M., Salleh, E., Adam, N. M., Sopian, A. R., & Yusof Sulaiman, M. (2010). Enhancement of stack ventilation in hot and humid climate using a combination of roof solar collector and vertical stack. *Building and Environment*, 45(10), 2296-2308.
- Zhai, X. Q., Dai, Y. J., & Wang, R. Z. (2005). Experimental investigation on air heating and natural ventilation of a solar air collector. *Energy and Buildings*, 37(4), 373-381.